Chapter 3
Straight and Curved Beams

Beams, plates and shells are commonly utilized in engineering applications, and they are named according to their size or/and shape characteristics and different theories have been developed to study their structural behaviors. A beam is typically described as a structural component having one dimension relatively greater than the other dimensions. Specially, a beam can be referred to as a rod or bar when subjected to tension, a column when subjected to compression and a shaft when subjected to torsional loads (Qatu 2004). Beams are one of the most fundamental structural elements. Almost every machine contains one or more beam components, such as bridges, steel framed structures and building frames. In addition, many structures can be modeled at a preliminary level as beams. For example, spring boards, supports of a wind power generation can be treated as cantilever beams, and a span of an overhead viaduct or bridge can be viewed as a simply supported beam. In recent decades, laminated beams made from advanced composite materials are extensively used in many engineering applications where higher strength to weight ratio is desired, such as aircraft structures, space vehicles, turbo-machines, deep-sea equipment and other industrial applications. Researches on the vibration and dynamic analyses of laminated composite beams have been increasing rapidly in recent decades. A paper which reviewed most of the researches done in years (1989–2012) on the vibration analysis of composite beams by Hajianmaleki and Qatu (2013) showed that research articles on the subject during period 2000–2012 are more than twice than those of 1989–2000. Due to the great importance, this chapter considers the vibration of laminated beams in the framework of classical thin beam theory (CBT) and shear deformation beam theory (SDBT).

Beams can be straight or curved. Both straight and curved beams are considered in this chapter. Generally, a straight beam can be considered as a degenerated curved beam with infinite radius of curvature (zero curvature). This chapter is concerned with the development of the fundamental equations of laminated curved beams according to the CBT and SDBT. Equations for the straight beams can be derived by setting curvatures to zero in those of curved beams. Strain-displacement relations, force and moment resultants, energy functions, governing equations and boundary conditions are derived and shown for both theories. Natural frequencies and mode shapes are presented for straight and curved beams with different boundary

© Science Press, Beijing and Springer-Verlag Berlin Heidelberg 2015

G. Jin et al., *Structural Vibration*, DOI 10.1007/978-3-662-46364-2_3

conditions, lamination schemes and geometry parameters in both strong and weak forms of the proposed modified Fourier series method. The effects of boundary conditions, geometry parameters and material properties are studied as well.

3.1 Fundamental Equations of Thin Laminated Beams

Fundamental equations of laminated thin beams are presented in this section in the framework of classical beam theory. As shown in Fig. 3.1, a laminated curved beam with uniform thickness h, width b is selected as the model. The beam is characterized by its middle surface, in which R represents the mean radius of the beam and θ_0 denotes the included angle of the curved beam. To describe the beam clearly, we introduce the following coordinate system: the α-coordinate is taken along the length of the beam, and β- and z-coordinates are taken along the width and the thickness directions, respectively. u, v and w separately indicate the middle surface displacement variations of the beam in the α, β and z directions. It should be stressed that this chapter addresses vibrations of laminated beams in their plane of curvature, therefore, the fundamental equations derived for thin deep shells can be specialized to those for curved beams by further assuming that the displacement v is identical with zero and the displacements u and w along the coordinate system are only functions of the α- and z-coordinates.

3.1.1 Kinematic Relations

Letting $\alpha = \theta$, the Lamé parameters of laminated curved beams can be obtained as $A = R$. Introducing the Lamé parameters into Eq. (1.7), the middle surface strain and curvature change of thin beams are:

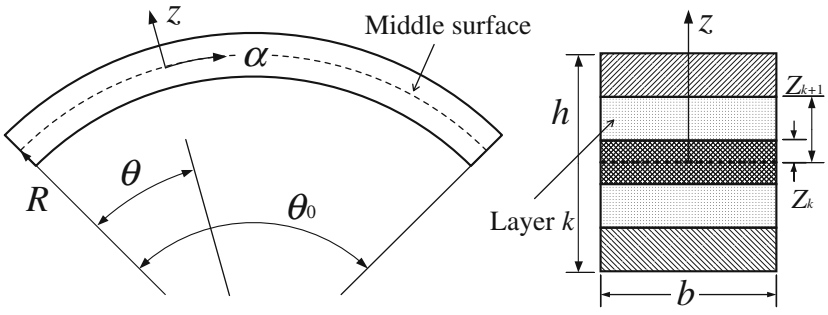

Fig. 3.1 Laminated curved beams

$$\varepsilon_\theta^0 = \frac{\partial u}{R\partial\theta} + \frac{w}{R} \quad \chi_\theta = \frac{\partial u}{R^2\partial\theta} - \frac{\partial^2 w}{R^2\partial\theta^2} \tag{3.1}$$

According to the thin beam assumption, the strain at an arbitrary point in the kth layer of thin laminated beams can be defined as:

$$\varepsilon_\theta = \varepsilon_\theta^0 + z\chi_\theta \tag{3.2}$$

where $Z_k < z < Z_{k+1}$. Z_{k+1} and Z_k denote the distances from the top surface and the bottom surface of the layer to the referenced middle surface, respectively.

3.1.2 Stress-Strain Relations and Stress Resultants

Suppose the laminated thin beam is composed of N composite layers which are bonded together rigidly. And the angle between the principal direction of the composite material in kth layer and the α axis is denoted by ϑ^k. According to Hooke's law, the corresponding stress-strain relations in the kth layer of the beam can be written as:

$$\{\sigma_\theta\}_k = \overline{Q_{11}^k}\{\varepsilon_\theta\}_k \tag{3.3}$$

where σ_θ is the normal stress in the θ direction. The constant $\overline{Q_{11}^k}$ is the elastic stiffness coefficient of this layer, which is found from following equations:

$$\begin{aligned} \overline{Q_{11}^k} &= Q_{11}^k \cos^4 \vartheta^k \\ Q_{11}^k &= \frac{E_1}{1 - \mu_{12}\mu_{21}} \end{aligned} \tag{3.4}$$

where E_1 is modulus of elasticity of the composite material in the principal direction. μ_{12} and μ_{21} are the Poisson's ratios. The subscript (11) in Eqs. (3.3) and (3.4) can be omitted but is maintained here for the direct use and comparison with the thin shell equations presented in Chap. 1. By carrying the integration of the normal stress over the cross-section results in

$$N_\theta = b\int_{-h/2}^{h/2} \sigma_\alpha dz \quad M_\theta = b\int_{-h/2}^{h/2} \sigma_\alpha z dz \tag{3.5}$$

where N_θ is the force resultant and M_θ is the moment resultant. The force and moment resultant relations to the strains in the middle surface and curvature change are defined as

$$\begin{bmatrix} N_\theta \\ M_\theta \end{bmatrix} = \begin{bmatrix} A_{11} & B_{11} \\ B_{11} & D_{11} \end{bmatrix} \begin{bmatrix} \varepsilon_\theta^0 \\ \chi_\theta \end{bmatrix} \tag{3.6}$$

where A_{11}, B_{11}, and D_{11} are the stiffness coefficients arising from the piecewise integration over the beam thickness:

$$\begin{aligned} A_{11} &= b \sum_{k=1}^{N} \overline{Q_{11}^k}(z_{k+1} - z_k) \\ B_{11} &= \tfrac{b}{2} \sum_{k=1}^{N} \overline{Q_{11}^k}(z_{k+1}^2 - z_k^2) \\ D_{11} &= \tfrac{b}{3} \sum_{k=1}^{N} \overline{Q_{11}^k}(z_{k+1}^3 - z_k^3) \end{aligned} \tag{3.7}$$

Notably, when the beam is laminated symmetrically with respect to its middle surface, the constants B_{ij} equal to zero. The above equations are valid for cylindrical bending of beams (Qatu 2004).

3.1.3 Energy Functions

The strain energy (U_s) of a thin beam during vibration is defined in terms of the middle surface strains and stress resultants as:

$$U_s = \frac{1}{2} \int_\theta \left\{ N_\theta \varepsilon_\theta^0 + M_\theta \chi_\theta \right\} R d\theta \tag{3.8}$$

Substituting Eqs. (3.1) and (3.6) into Eq. (3.8), the strain energy of the beam can be rewritten in terms of the displacements as:

$$U_s = \frac{1}{2} \int_\theta \left\{ \begin{array}{c} A_{11} \left(\dfrac{\partial u}{R \partial \theta} + \dfrac{w}{R} \right)^2 + D_{11} \left(\dfrac{\partial u}{R^2 \partial \theta} - \dfrac{\partial^2 w}{R^2 \partial \theta^2} \right)^2 \\ + 2B_{11} \left(\dfrac{\partial u}{R^2 \partial \theta} - \dfrac{\partial^2 w}{R^2 \partial \theta^2} \right) \left(\dfrac{\partial u}{R \partial \theta} + \dfrac{w}{R} \right) \end{array} \right\} R d\theta \tag{3.9}$$

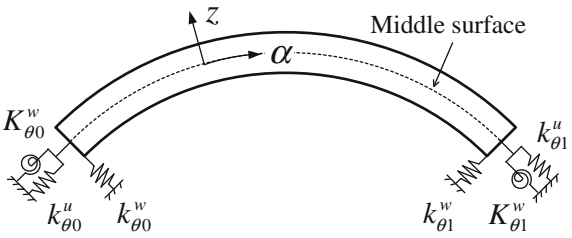

Fig. 3.2 Boundary conditions of thin laminated beams

The kinetic energy (T) of the beam is written as:

$$T = \frac{1}{2}\int_{\theta} I_0 \left\{ \left(\frac{\partial u}{\partial t}\right)^2 + \left(\frac{\partial w}{\partial t}\right)^2 \right\} R d\theta \tag{3.10}$$

where the inertia term are:

$$I_0 = b\sum_{k=1}^{N}\int_{z_k}^{z_{k+1}} \rho^k dz \tag{3.11}$$

ρ^k is the mass of the kth layer per unit middle surface area. The external work is expressed as:

$$W_e = \int_{\theta} \{q_\theta u + q_z w\} R d\theta \tag{3.12}$$

where q_θ and q_z are the external loads in the θ and z directions, respectively.

As described earlier, the general boundary conditions of a beam are implemented by using the artificial spring boundary technique, in which each end of the beam is assumed to be restrained by two groups of linear springs (k_u and k_w) and one group of rotational springs (K_w) to simulate the given or typical boundary conditions expressed in the form of boundary forces and the flexural moments, respectively (see Fig. 3.2). Specifically, symbols k^u_ψ, k^w_ψ and K^w_ψ ($\psi = \theta_0$ and θ_1) are used to indicate the stiffness of the boundary springs at the boundaries $\theta = 0$ and $\theta = \theta_0$, respectively. Therefore, the deformation strain energy (U_{sp}) stored in the boundary springs can be written as:

$$U_{sp} = \frac{1}{2}\left\{ \begin{array}{l} \left[k^u_{\theta 0}u^2 + k^w_{\theta 0}w^2 + K^w_{\theta 0}(\partial w/R\partial\theta)^2\right]_{\theta=0} \\ +\left[k^u_{\theta 1}u^2 + k^w_{\theta 1}w^2 + K^w_{\theta 1}(\partial w/R\partial\theta)^2\right]_{\theta=\theta_0} \end{array} \right\} \tag{3.13}$$

3.1.4 Governing Equations and Boundary Conditions

The governing equations and boundary conditions of thin laminated beams can be obtained by specializing the governing equations of thin shells to those of thin laminated beams (i.e. substituting $\alpha = \theta$, $A = R$, $B = 1$ and $R_\alpha = R$ into Eq. (1.28) and deleting all the terms with respect to β). According to Eq. (1.28), the governing equations are:

$$\begin{aligned} \frac{\partial N_\theta}{R\partial\theta} + \frac{Q_\theta}{R} + q_\theta &= I_0 \frac{\partial^2 u}{\partial t^2} \\ -\frac{N_\theta}{R} + \frac{\partial Q_\theta}{R\partial\theta} + q_z &= I_0 \frac{\partial^2 w}{\partial t^2} \end{aligned} \tag{3.14}$$

where

$$Q_\theta = \frac{\partial M_\theta}{R\partial\theta} \tag{3.15}$$

And the general boundary conditions of thin laminated beams are

$$\theta = 0 : \begin{cases} N_\theta + \frac{M_\theta}{R} - k_{\theta 0}^u u = 0 \\ Q_\theta - k_{\theta 0}^w w = 0 \\ -M_\theta - K_{\theta 0}^w \frac{\partial w}{R\partial\theta} = 0 \end{cases} \quad \theta = \theta_0 : \begin{cases} N_\theta + \frac{M_\theta}{R} + k_{\theta 1}^u u = 0 \\ Q_\theta + k_{\theta 1}^w w = 0 \\ -M_\theta + K_{\theta 1}^w \frac{\partial w}{R\partial\theta} = 0 \end{cases} \tag{3.16}$$

Alternately, the governing equations and boundary conditions of the considered beam can be obtained by applying Hamilton's principle in the same manner as following describe. The Lagrangian function (L) of thin laminated beams can be expressed in terms of strain energy, kinetic energy and external work as:

$$L = T - U_s - U_{sp} + W_e \tag{3.17}$$

Substituting Eqs. (3.9), (3.10), (3.12) and (3.13) into Eq. (3.17) and applying Hamilton's principle:

$$\delta \int_0^t \left(T - U_s - U_{sp} + W_e\right) dt = 0 \tag{3.18}$$

yields:

$$\begin{aligned}
&\int_0^t \int_\theta \left\{ I_0 \left(\frac{\partial u}{\partial t}\frac{\partial \delta u}{\partial t} + \frac{\partial w}{\partial t}\frac{\partial \delta w}{\partial t} \right) + q_\theta \delta u + q_z \right\} R d\theta dt \\
&\quad = \int_0^t \int_\theta \left\{ N_\theta \left(\frac{\partial \delta u}{\partial \theta} + \delta w \right) + M_\theta \left(\frac{\partial \delta u}{R\partial \theta} - \frac{\partial^2 \delta w}{R\partial \theta^2} \right) \right\} d\theta dt \\
&\qquad + \int_0^t \left\{ \begin{array}{l} \left[k_{\theta 0}^u u \delta u + k_{\theta 0}^w w \delta w + K_{\theta 0}^w \dfrac{\partial w}{R\partial \theta}\dfrac{\partial \delta w}{R\partial \theta} \right]_{\theta=0} \\ + \left[k_{\theta 1}^u u \delta u + k_{\theta 1}^w w \delta w + K_{\theta 1}^w \dfrac{\partial w}{R\partial \theta}\dfrac{\partial \delta w}{R\partial \theta} \right]_{\theta=\theta_0} \end{array} \right\} dt
\end{aligned} \tag{3.19}$$

Integrating by parts to relieve the virtual displacements δu and δw, we have

$$\begin{aligned}
0 = &\int_0^t \int_\theta \left\{ \frac{\partial N_\theta}{\partial \theta} + R\left(\frac{Q_\theta}{R} + q_\theta - I_0 \frac{\partial^2 u}{\partial t^2} \right) \right\} \delta u d\theta dt \\
&+ \int_0^t \int_\theta \left\{ -N_\theta + \frac{\partial Q_\theta}{\partial \theta} + R\left(q_z - I_0 \frac{\partial^2 w}{\partial t^2} \right) \right\} \delta w d\theta dt \\
&- \int_0^t \left\{ \begin{array}{l} \left(N_\theta + \dfrac{M_\theta}{R} + k_{\theta 1}^u u \right) \delta u|_{\theta_0} - \left(N_\theta + \dfrac{M_\theta}{R} - k_{\theta 0}^u u \right) \delta u|_0 \\ + \left(-M_\theta + K_{\theta 1}^w \dfrac{\partial w}{R\partial \theta} \right) \dfrac{\partial \delta w}{R\partial \theta}|_{\theta_0} + \left(Q_\theta + k_{\theta 1}^w w \right) \delta w|_{\theta_0} \\ + \left(M_\theta + K_{\theta 0}^w \dfrac{\partial w}{R\partial \theta} \right) \dfrac{\partial \delta w}{R\partial \theta}|_0 - \left(Q_\theta - k_{\theta 0}^w w \right) \delta w|_0 \end{array} \right\} dt
\end{aligned} \tag{3.20}$$

Since the virtual displacements δu and δw are arbitrary, the Eq. (3.20) can be satisfied only is the coefficients of the virtual displacements are zero. Thus, the governing equations and boundary conditions of thin laminated beams are obtained, which is the same as those presented in Eqs. (3.14) and (3.16). For general curved beams and asymmetrically laminated straight beams, each boundary can exist two possible combinations for each type of classical boundary conditions (free, simply-supported, and clamped). At each boundary of θ = constant, the possible combinations for each classical boundary condition are given in Table 3.1.

By using the artificial spring boundary technique, taking edge $\theta = 0$ for example, the F, S (simply-supported), SD (shear-diaphragm) and C (completely clamped) boundary conditions which are of particular interest can be readily realized by assigning the stiffness of the boundary springs at proper values as follows:

Table 3.1 Possible classical boundary conditions for thin laminated curved beams

Boundary type	Conditions
Free boundary conditions	
F	$N_\theta + \frac{M_\theta}{R_\theta} = Q_\theta = M_\theta = 0$
F2	$u = Q_\theta = M_\theta = 0$
Simply supported boundary conditions	
S	$u = w = M_\theta = 0$
SD	$N_\theta + \frac{M_\theta}{R_\theta} = w = M_\theta = 0$
Clamped boundary conditions	
C	$u = w = \frac{\partial w}{R\partial\theta} = 0$
C2	$N_\theta + \frac{M_\theta}{R_\theta} = w = \frac{\partial w}{R\partial\theta} = 0$

$$\begin{aligned} \text{F}: &\ k_{\theta 0}^{u} = k_{\theta 0}^{w} = K_{\theta 0}^{w} = 0 \\ \text{SD}: &\ k_{\theta 0}^{w} = 10^{7}D,\ k_{\theta 0}^{u} = K_{\theta 0}^{w} = 0 \\ \text{S}: &\ k_{\theta 0}^{u} = k_{\theta 0}^{w} = 10^{7}D,\ K_{\theta 0}^{w} = 0 \\ \text{C}: &\ k_{\theta 0}^{u} = k_{\theta 0}^{w} = K_{\theta 0}^{w} = 10^{7}D \end{aligned} \tag{3.21}$$

where $D = E_1 h^3/12(1 - \mu_{12}\mu_{21})$ is the flexural stiffness of the beam.

Figure 3.3 shows the variations of the fundamental frequency parameters $\Delta\Omega$ (where $\Delta\Omega$ is defined as the difference of the fundamental frequency to that of the elastic restraint parameter $\Gamma = 10^{-3}$, namely, $\Delta\Omega = f(\Gamma) - f(10^{-3}D)$) versus restraint parameter Γ of a steel (E = 210 GPa, μ = 0.3, ρ = 7800 kg/m^3) thin curved beam with different geometry parameters. The beam is clamped at boundary $\theta = \theta_0$ and elastically supported at boundary $\theta = 0$ (i.e., $k_{\theta 0}^{u} = k_{\theta 0}^{w} = K_{\theta 0}^{w} = \Gamma D$). According to Fig. 3.3, we can see that the change of the restraint parameter Γ has little effect on

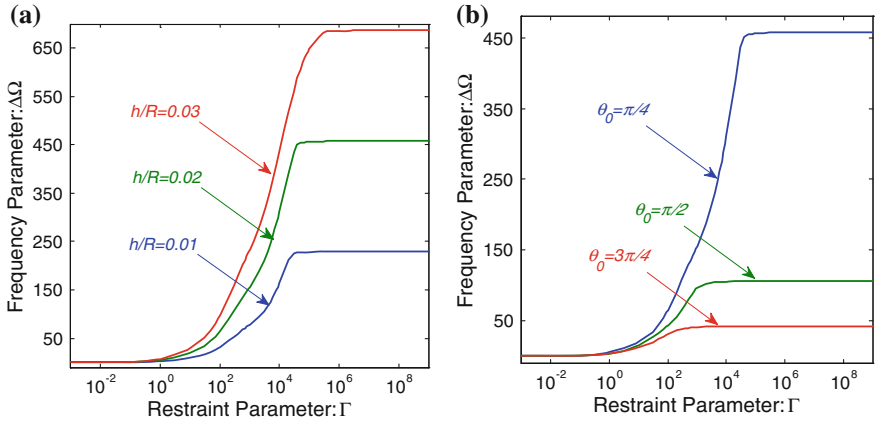

Fig. 3.3 Variation of fundamental frequency parameter $\Delta\Omega$ versus elastic restraint parameters Γ for a *thin* beam (R = 1) with different geometry parameters (a) $\theta_0 = \pi/4$; (b) h/R = 0.02

frequency parameter $\Delta\Omega$ when it is smaller than 10^0. However, when it is increased from 10^0 to 10^5, the frequency parameters increase rapidly. Then, the frequency parameters approach their utmost and remain unchanged when Γ approaches infinity. In such a case, the beam can be deemed as clamped in both ends. In conclusion, by assigning the stiffness of the boundary springs at $10^7 D$, the completely clamped boundary conditions of a beam can be realized.

3.2 Fundamental Equations of Thick Laminated Beams

In the CBT, the effects of shear deformation and rotary inertia are neglected. It is only applicable for thin beams. For beams with higher thickness ratios, the assumption that normals to the undeformed middle surface remain straight and normal to the deformed middle surface and suffer no extension of the classical beam theory should be relaxed and both shear deformation and rotary inertia effects should be included in the calculation. In this section, fundamental equations of laminated beams in the framework of shear deformation beam theory are developed and the deepness term $(1 + z/R_\alpha)$ is considered in the formulation.

3.2.1 Kinematic Relations

Assuming that normals to the undeformed middle surface remain straight but not normal to the deformed middle surface, the displacement field in the beam space can be expressed in terms of middle surface displacements and rotation component as:

$$U(\theta, z) = u(\theta) + z\phi_\theta(\theta), \quad W(\theta, z) = w(\theta) \tag{3.22}$$

where u and w are the displacements at the middle surface in the θ and z directions. ϕ_θ represents the rotation of transverse normal, see Fig. 3.1. Letting $\alpha = \theta$, $A = R$ and $R_\alpha = R$ and specializing Eqs. (1.33) and (1.34) to those of beams, the normal and shear strains at any point of the beam space can be defined in terms of middle surface strains and curvature change as:

$$\begin{aligned} \varepsilon_\theta &= \frac{1}{(1 + z/R)}\left(\varepsilon_\theta^0 + z\chi_\theta\right) \\ \gamma_{\theta z} &= \frac{1}{(1 + z/R)}\gamma_{\theta z}^0 \end{aligned} \tag{3.23}$$

where ε_θ^0 and $\gamma_{\theta z}^0$ denote the normal and shear strains in the reference surface. χ_θ is the curvature change. They are defined in terms of the middle surface displacements and rotation component as:

$$\begin{aligned} \varepsilon_\theta^0 &= \frac{\partial u}{R\partial\theta} + \frac{w}{R}, \quad \chi_\theta = \frac{\partial \phi_\theta}{R\partial\theta} \\ \gamma_{\theta z}^0 &= \frac{\partial w}{R\partial\theta} - \frac{u}{R} + \phi_\theta \end{aligned} \tag{3.24}$$

3.2.2 Stress-Strain Relations and Stress Resultants

According to Hooke's law, the corresponding stress-strain relations in the kth layer of thick laminated curved beams can be written as:

$$\begin{Bmatrix} \sigma_\theta \\ \tau_{\theta z} \end{Bmatrix}_k = \begin{bmatrix} \overline{Q_{11}^k} & 0 \\ 0 & \overline{Q_{55}^k} \end{bmatrix} \begin{Bmatrix} \varepsilon_\theta \\ \gamma_{\theta z} \end{Bmatrix}_k \tag{3.25}$$

where σ_θ represents the normal stress, $\tau_{\theta z}$ is the shear stress. The elastic stiffness coefficients $\overline{Q_{ii}^k}$ (i = 1, 5) are defined by following equations:

$$\begin{aligned} &\overline{Q_{11}^k} = Q_{11}^k \cos^4 \vartheta^k \quad \text{and} \quad Q_{11}^k = \frac{E_1}{1 - \mu_{12}\mu_{21}} \\ &\overline{Q_{55}^k} = Q_{55}^k \cos^2 \vartheta^k \quad \text{and} \quad Q_{55}^k = G_{13} \end{aligned} \tag{3.26}$$

where E_1 is the modulus of elasticity of the composite material in the principal direction. μ_{12} and μ_{21} are the Poisson's ratios. G_{13} is the shear modulus. ϑ^k represents the included angle between the principal direction of the layer and the θ-axis. By carrying the integration of the normal stress over the cross-section, the force and moment resultants can be obtained:

$$\begin{bmatrix} N_\theta \\ Q_\theta \end{bmatrix} = b \int_{-h/2}^{h/2} \begin{bmatrix} \sigma_\theta \\ \tau_{\theta z} \end{bmatrix} dz \quad M_\theta = b \int_{-h/2}^{h/2} \sigma_\theta z dz \tag{3.27}$$

where Q_θ represents the transverse shear force resultant. Performing the integration operation in Eq. (3.27), the force and moment resultants can be written in terms of the middle surface strains and curvature change as:

$$\begin{bmatrix} N_\theta \\ M_\theta \\ Q_\theta \end{bmatrix} = \begin{bmatrix} A_{11} & B_{11} & 0 \\ B_{11} & D_{11} & 0 \\ 0 & 0 & A_{55} \end{bmatrix} \begin{bmatrix} \varepsilon_\theta^0 \\ \chi_\theta \\ \gamma_{\theta z}^0 \end{bmatrix} \tag{3.28}$$

The stiffness coefficients A_{11}, A_{55}, B_{11} and D_{11} are defined as follows:

$$\begin{aligned}
A_{11} &= Rb\sum_{k=1}^{N}\overline{Q_{11}^{k}}\ln\left(\frac{R+z_{k+1}}{R+z_k}\right)\\
A_{55} &= K_sRb\sum_{k=1}^{N}\overline{Q_{55}^{k}}\ln\left(\frac{R+z_{k+1}}{R+z_k}\right)\\
B_{11} &= Rb\sum_{k=1}^{N}\overline{Q_{11}^{k}}\left[(z_{k+1}-z_k)-R\ln\left(\frac{R+z_{k+1}}{R+z_k}\right)\right]\\
D_{11} &= Rb\sum_{k=1}^{N}\overline{Q_{11}^{k}}\left[\frac{1}{2}\left(z_{k+1}^2-z_k^2\right)-2R(z_{k+1}-z_k)+R^2\ln\left(\frac{R+z_{k+1}}{R+z_k}\right)\right]
\end{aligned} \tag{3.29}$$

in which K_s is the shear correction factor, typically taken at 5/6 (Qatu 2004; Reddy 2003).

3.2.3 Energy Functions

The strain energy (U_s) of thick laminated curved beams during vibration can be defined as

$$U_s = \frac{1}{2}\int_{\theta}\left\{N_\theta\varepsilon_\theta^0+M_\theta\chi_\theta+Q_\theta\gamma_{\theta z}^0\right\}Rd\theta \tag{3.30}$$

Substituting Eqs. (3.24) and (3.28) into Eq. (3.30), the strain energy function of thick curved beams can be rewritten as:

$$U_s = \frac{1}{2}\int_{\theta}\left\{\begin{array}{l}A_{11}\left(\frac{\partial u}{R\partial\theta}+\frac{w}{R}\right)^2+2B_{11}\frac{\partial\phi_\theta}{R\partial\theta}\left(\frac{\partial u}{R\partial\theta}+\frac{w}{R}\right)\\ +D_{11}\left(\frac{\partial\phi_\theta}{R\partial\theta}\right)^2+A_{55}\left(\frac{\partial w}{R\partial\theta}-\frac{u}{R}+\phi_\theta\right)^2\end{array}\right\}Rd\theta \tag{3.31}$$

The corresponding kinetic energy (T) function of the beams is written as:

$$T = \frac{1}{2}\int_{\theta}\left\{\overline{I_0}\left(\frac{\partial u}{\partial t}\right)^2+2\overline{I_1}\frac{\partial u}{\partial t}\frac{\partial\phi_\theta}{\partial t}+\overline{I_2}\left(\frac{\partial\phi_\theta}{\partial t}\right)^2+\overline{I_0}\left(\frac{\partial w}{\partial t}\right)^2\right\}Rd\theta \tag{3.32}$$

where the inertia terms are defined as:

$$\begin{aligned}\overline{I_0}&=I_0+\frac{I_1}{R}\\ \overline{I_1}&=I_1+\frac{I_2}{R}\\ \overline{I_2}&=I_2+\frac{I_3}{R}\\ [I_0,I_1,I_2,I_3]&=b\sum_{k=1}^{N}\int_{z_k}^{z_{k+1}}\rho^k[1,z,z^2,z^3]dz\end{aligned}\tag{3.33}$$

in which ρ^k is the mass of the k'th layer per unit middle surface area. The external work is expressed as:

$$W_e=\int_{\theta}\{q_\theta u+q_z w+m_\theta\phi_\theta\}Rd\theta\tag{3.34}$$

where q_θ and q_z denote the external loads. m_θ is the external couples in the middle surface of the beam. Using the artificial spring boundary technique similar to that described earlier, symbols k_ψ^u, k_ψ^w and K_ψ^θ ($\psi = \theta_0$ and θ_1) are used to indicate the rigidities (per unit length) of the boundary springs at the boundaries $\theta = 0$ and $\theta = \theta_0$, respectively, see Fig. 3.4. Therefore, the deformation strain energy (U_{sp}) stored in the boundary springs during vibration can be defined as:

$$U_{sp}=\frac{1}{2}\left\{\left[k_{\theta0}^u u^2+k_{\theta0}^w w^2+K_{\theta0}^\theta\phi_\theta^2\right]_{\theta=0}+\left[k_{\theta1}^u u^2+k_{\theta1}^w w^2+K_{\theta1}^\theta\phi_\theta^2\right]_{\theta=\theta_0}\right\}\tag{3.35}$$

3.2.4 Governing Equations and Boundary Conditions

Specializing the governing equations and boundary conditions of the thick shell (Eq. 1.59) to those of thick beams, we have

$$\begin{aligned}\frac{\partial N_\theta}{R\partial\theta}+\frac{Q_\theta}{R}+q_\theta&=\overline{I_0}\frac{\partial^2 u}{\partial t^2}+\overline{I_1}\frac{\partial^2\phi_\theta}{\partial t^2}\\ -\frac{N_\theta}{R}+\frac{\partial Q_\theta}{R\partial\theta}+q_z&=\overline{I_0}\frac{\partial^2 w}{\partial t^2}\\ \frac{\partial M_\theta}{R\partial\theta}-Q_\theta+m_\theta&=\overline{I_1}\frac{\partial^2 u}{\partial t^2}+\overline{I_2}\frac{\partial^2\phi_\theta}{\partial t^2}\end{aligned}\tag{3.36}$$

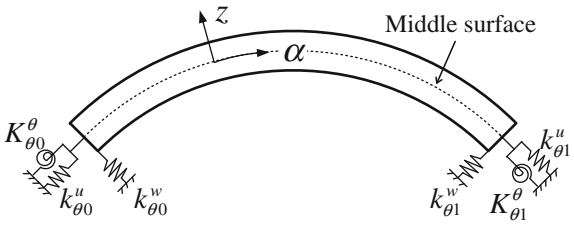

Fig. 3.4 Boundary conditions of a *thick* laminated beam

Similarly, according to Eq. (1.60), the general boundary conditions of thick laminated curved beams are written as:

$$\theta = 0: \begin{cases} N_\theta - k^u_{\theta 0} u = 0 \\ Q_\theta - k^w_{\theta 0} w = 0 \\ M_\theta - K^\theta_{\theta 0} \phi_\theta = 0 \end{cases}, \quad \theta = \theta_0: \begin{cases} N_\theta + k^u_{\theta 1} u = 0 \\ Q_\theta + k^w_{\theta 1} w = 0 \\ M_\theta + K^\theta_{\theta 1} \phi_\theta = 0 \end{cases} \tag{3.37}$$

Alternately, the governing equations and boundary conditions for the thick beams can be obtained by applying Hamilton's principle in the same manner as described in Sect. 3.1.4.

For thick curved beams or unsymmetrically laminated straight beams, each boundary exits two possible combinations for each classical boundary condition. At each boundary, the possible combinations for each classical boundary condition are given in Table 3.2.

In the framework of artificial spring boundary technique, taking edge $\theta = 0$ for example, the frequently encountered boundary conditions F, S, SD and C can be readily realized by assigning the stiffness of the boundary springs at proper values as follows:

Table 3.2 Possible classical boundary conditions for thick curved beams

Boundary type	Conditions
Free boundary conditions	
F	$N_\theta = Q_\theta = M_\theta = 0$
F2	$u = Q_\theta = M_\theta = 0$
Simply supported boundary conditions	
S	$u = w = M_\theta = 0$
SD	$N_\theta = w = M_\theta = 0$
Clamped boundary conditions	
C	$u = w = \phi_\theta = 0$
C2	$N_\theta = w = \phi_\theta = 0$

$$\begin{aligned}
\text{F}: &\quad k_{\theta 0}^{u} = k_{\theta 0}^{w} = K_{\theta 0}^{\theta} = 0 \\
\text{SD}: &\quad k_{\theta 0}^{w} = 10^{7}D,\ k_{\theta 0}^{u} = K_{\theta 0}^{\theta} = 0 \\
\text{S}: &\quad k_{\theta 0}^{u} = k_{\theta 0}^{w} = 10^{7}D,\ K_{\theta 0}^{\theta} = 0 \\
\text{C}: &\quad k_{\theta 0}^{u} = k_{\theta 0}^{w} = K_{\theta 0}^{\theta} = 10^{7}D
\end{aligned} \tag{3.38}$$

3.3 Solution Procedures

With above fundamental equations and modified Fourier series method developed in Chap. 2, both strong and weak form solution procedures of laminated beams with general boundary conditions are presented in this section. To fully illustrate the modified Fourier series solution procedure, we only consider the free vibration analysis of laminated beams with general boundary conditions based on the SDBT. For other beam theories, the corresponding solution procedures can be obtained in the same manner.

Combining Eqs. (3.24), (3.28) and (3.36), it is obvious that the displacements and rotation components of thick laminated curved beams are required to have up to the second derivative. Therefore, regardless of boundary conditions, each displacements and rotation component of a laminated beam can be expanded as a one-dimensional modified Fourier series as

$$\begin{aligned}
u(\theta) &= \sum_{m=0}^{M} A_m \cos \lambda_m \theta + a_1 P_1(\theta) + a_2 P_2(\theta) \\
w(\theta) &= \sum_{m=0}^{M} B_m \cos \lambda_m \theta + b_1 P_1(\theta) + b_2 P_2(\theta) \\
\phi_\theta(\theta) &= \sum_{m=0}^{M} C_m \cos \lambda_m \theta + c_1 P_1(\theta) + c_2 P_2(\theta)
\end{aligned} \tag{3.39}$$

where $\lambda_m = m\pi/\theta_0$. $P_1(\theta)$ and $P_2(\theta)$ denote the auxiliary polynomial functions introduced to remove all the discontinuities potentially associated with the first-order derivatives at the boundaries then ensure and accelerate the convergence of the series expansion of the beam displacements and rotation component. M is the truncation number. A_m, B_m and C_m are the expansion coefficients of standard cosine Fourier series. a_1, a_2, b_1, b_2, c_1 and c_2 represent the corresponding expansion coefficients of auxiliary functions $P_1(\theta)$ and $P_2(\theta)$. These two auxiliary functions are defined as

$$P_1(\theta) = \theta\left(\frac{\theta}{\theta_0} - 1\right)^2 \quad P_2(\theta) = \frac{\theta^2}{\theta_0}\left(\frac{\theta}{\theta_0} - 1\right) \tag{3.40}$$

It should be stressed that in the CBT cases, the displacements of a laminated beam are required to have up to the fourth-order derivatives. In such case, the following four auxiliary polynomial functions are introduced to remove all the discontinuities potentially associated with the first-order and third-order derivatives at the boundaries (Jin et al. 2013a).

$$\begin{aligned} P_1(\theta) &= \frac{9\theta_0}{4\pi}\sin(\frac{\pi\theta}{2\theta_0}) - \frac{\theta_0}{12\pi}\sin(\frac{3\pi\theta}{2\theta_0}) \\ P_2(\theta) &= -\frac{9\theta_0}{4\pi}\cos(\frac{\pi\theta}{2\theta_0}) - \frac{\theta_0}{12\pi}\cos(\frac{3\pi\theta}{2\theta_0}) \\ P_3(\theta) &= \frac{\theta_0^3}{\pi^3}\sin(\frac{\pi\theta}{2\theta_0}) - \frac{\theta_0^3}{3\pi^3}\sin(\frac{3\pi\theta}{2\theta_0}) \\ P_4(\theta) &= -\frac{\theta_0^3}{\pi^3}\cos(\frac{\pi\theta}{2\theta_0}) - \frac{\theta_0^3}{3\pi^3}\cos(\frac{3\pi\theta}{2\theta_0}) \end{aligned} \tag{3.41}$$

3.3.1 Strong Form Solution Procedure

Substituting Eqs. (3.24) and (3.28) into Eq. (3.36) the governing equations of laminated curved beams including shear deformation and rotary inertia effects can be rewritten as:

$$\left(\begin{bmatrix} L_{11} & L_{12} & L_{13} \\ L_{21} & L_{22} & L_{23} \\ L_{31} & L_{32} & L_{33} \end{bmatrix} - \omega^2 \begin{bmatrix} M_{11} & 0 & M_{13} \\ 0 & M_{22} & 0 \\ M_{31} & 0 & M_{33} \end{bmatrix} \right) \begin{bmatrix} u \\ w \\ \phi_\theta \end{bmatrix} = \begin{bmatrix} 0 \\ 0 \\ 0 \end{bmatrix} \tag{3.42}$$

where the coefficients of the linear operator ($M_{ij} = M_{ji}$) are given below:

$$\begin{aligned} L_{11} &= \frac{A_{11}}{R^2}\frac{\partial^2}{\partial\theta^2} - \frac{A_{55}}{R^2}, & L_{12} &= \frac{A_{11}}{R^2}\frac{\partial}{\partial\theta} + \frac{A_{55}}{R^2}\frac{\partial}{\partial\theta} \\ L_{13} &= \frac{B_{11}}{R^2}\frac{\partial^2}{\partial\theta^2} + \frac{A_{55}}{R}, & L_{21} &= -\frac{A_{11}}{R^2}\frac{\partial}{\partial\theta} - \frac{A_{55}}{R^2}\frac{\partial}{\partial\theta} \\ L_{22} &= -\frac{A_{11}}{R^2} + \frac{A_{55}}{R^2}\frac{\partial^2}{\partial\theta^2}, & L_{23} &= -\frac{B_{11}}{R^2}\frac{\partial}{\partial\theta} + \frac{A_{55}}{R}\frac{\partial}{\partial\theta} \\ L_{31} &= \frac{B_{11}}{R^2}\frac{\partial^2}{\partial\theta^2} + \frac{A_{55}}{R}, & L_{32} &= \frac{B_{11}}{R^2}\frac{\partial}{\partial\theta} - \frac{A_{55}}{R}\frac{\partial}{\partial\theta} \\ L_{33} &= \frac{D_{11}}{R^2}\frac{\partial^2}{\partial\theta^2} - A_{55}, & M_{11} &= M_{22} = -\overline{I_0} \\ M_{13} &= M_{31} = -\overline{I_1}, & M_{33} &= -\overline{I_2} \end{aligned} \tag{3.43}$$

Rewriting the modified Fourier series expressions (Eq. 3.39) in the matrix form as:

$$\begin{aligned} u(\theta) &= \mathbf{H}_{sc}\mathbf{A}+\mathbf{H}_{af}\mathbf{a} \\ w(\theta) &= \mathbf{H}_{sc}\mathbf{B}+\mathbf{H}_{af}\mathbf{b} \\ \phi_\theta(\theta) &= \mathbf{H}_{sc}\mathbf{C}+\mathbf{H}_{af}\mathbf{c} \end{aligned} \tag{3.44}$$

where

$$\begin{aligned} \mathbf{H}_{sc} &= [\cos\lambda_0\theta,\ldots,\cos\lambda_m\theta,\ldots,\cos\lambda_M\theta] \\ \mathbf{H}_{af} &= [P_1(\theta),P_2(\theta)] \\ \mathbf{A} &= [A_0,\ldots,A_m,\ldots,A_M]^T \quad \mathbf{a} = [a_1,a_2]^T \\ \mathbf{B} &= [B_0,\ldots,B_m,\ldots,B_M]^T \quad \mathbf{b} = [b_1,b_2]^T \\ \mathbf{C} &= [C_0,\ldots,C_m,\ldots,C_M]^T \quad \mathbf{c} = [c_1,c_2]^T \end{aligned} \tag{3.45}$$

where superscript T represents the transposition operator. Substituting Eq. (3.44) into Eq. (3.42) results in

$$\mathbf{L}_{sc}\begin{bmatrix}\mathbf{A}\\ \mathbf{B}\\ \mathbf{C}\end{bmatrix}+\mathbf{L}_{af}\begin{bmatrix}\mathbf{a}\\ \mathbf{b}\\ \mathbf{c}\end{bmatrix}-\omega^2\left(\mathbf{M}_{sc}\begin{bmatrix}\mathbf{A}\\ \mathbf{B}\\ \mathbf{C}\end{bmatrix}+\mathbf{M}_{af}\begin{bmatrix}\mathbf{a}\\ \mathbf{b}\\ \mathbf{c}\end{bmatrix}\right)=\mathbf{0} \tag{3.46}$$

where

$$\begin{aligned} \mathbf{L}_i &= \begin{bmatrix} L_{11}\mathbf{H}_i & L_{12}\mathbf{H}_i & L_{13}\mathbf{H}_i \\ L_{21}\mathbf{H}_i & L_{22}\mathbf{H}_i & L_{23}\mathbf{H}_i \\ L_{31}\mathbf{H}_i & L_{32}\mathbf{H}_i & L_{33}\mathbf{H}_i \end{bmatrix} (i=sc,af) \\ \mathbf{M}_i &= \begin{bmatrix} M_{11}\mathbf{H}_i & \mathbf{0} & M_{13}\mathbf{H}_i \\ \mathbf{0} & M_{22}\mathbf{H}_i & \mathbf{0} \\ M_{31}\mathbf{H}_i & \mathbf{0} & M_{33}\mathbf{H}_i \end{bmatrix} (i=sc,af) \end{aligned} \tag{3.47}$$

Similarly, substituting Eq. (3.44) into Eq. (3.37), the boundary conditions of thick laminated curved beams can be rewritten as

$$\begin{bmatrix} \mathbf{L}_{sc}^{\theta 0} \\ \mathbf{L}_{sc}^{\theta 1} \end{bmatrix} \begin{bmatrix} \mathbf{A} \\ \mathbf{B} \\ \mathbf{C} \end{bmatrix} + \begin{bmatrix} \mathbf{L}_{af}^{\theta 0} \\ \mathbf{L}_{af}^{\theta 1} \end{bmatrix} \begin{bmatrix} \mathbf{a} \\ \mathbf{b} \\ \mathbf{c} \end{bmatrix} = \mathbf{0} \tag{3.48}$$

where

$$\mathbf{L}_i^{\theta 0} = \begin{bmatrix} \frac{A_{11}}{R}\frac{\partial \mathbf{H}_i}{\partial \theta} - k_{\theta 0}^{u}\mathbf{H}_i & \frac{A_{11}}{R}\mathbf{H}_i & \frac{B_{11}}{R}\frac{\partial \mathbf{H}_i}{\partial \theta} \\ -\frac{A_{55}}{R}\mathbf{H}_i & \frac{A_{55}}{R}\frac{\partial \mathbf{H}_i}{\partial \theta} - k_{\theta 0}^{w}\mathbf{H}_i & A_{55}\mathbf{H}_i \\ \frac{B_{11}}{R}\frac{\partial \mathbf{H}_i}{\partial \theta} & \frac{B_{11}}{R}\mathbf{H}_i & \frac{D_{11}}{R}\frac{\partial \mathbf{H}_i}{\partial \theta} - K_{\theta 0}^{\theta}\mathbf{H}_i \end{bmatrix}_{\theta=0} \quad (i = sc, af)$$

$$\mathbf{L}_i^{\theta 1} = \begin{bmatrix} \frac{A_{11}}{R}\frac{\partial \mathbf{H}_i}{\partial \theta} + k_{\theta 1}^{u}\mathbf{H}_i & \frac{A_{11}}{R}\mathbf{H}_i & \frac{B_{11}}{R}\frac{\partial \mathbf{H}_i}{\partial \theta} \\ -\frac{A_{55}}{R}\mathbf{H}_i & \frac{A_{55}}{R}\frac{\partial \mathbf{H}_i}{\partial \theta} + k_{\theta 1}^{w}\mathbf{H}_i & A_{55}\mathbf{H}_i \\ \frac{B_{11}}{R}\frac{\partial \mathbf{H}_i}{\partial \theta} & \frac{B_{11}}{R}\mathbf{H}_i & \frac{D_{11}}{R}\frac{\partial \mathbf{H}_i}{\partial \theta} + K_{\theta 1}^{\theta}\mathbf{H}_i \end{bmatrix}_{\theta=\theta_0} \quad (i = sc, af) \tag{3.49}$$

Thus, the relation between the expansion coefficients of standard cosine Fourier series (**A**, **B** and **C**) and those of corresponding auxiliary functions (**a**, **b** and **c**) can be determined by the following equation:

$$\begin{bmatrix} \mathbf{a} \\ \mathbf{b} \\ \mathbf{c} \end{bmatrix} = -\begin{bmatrix} \mathbf{L}_{af}^{\theta 0} \\ \mathbf{L}_{af}^{\theta 1} \end{bmatrix}^{-1} \begin{bmatrix} \mathbf{L}_{sc}^{\theta 0} \\ \mathbf{L}_{sc}^{\theta 1} \end{bmatrix} \begin{bmatrix} \mathbf{A} \\ \mathbf{B} \\ \mathbf{C} \end{bmatrix} \tag{3.50}$$

In order to derive the constraint equations for the unknown expansion coefficients, all the sine terms, the auxiliary polynomial functions and their derivatives in Eq. (3.46) are expanded into Fourier cosine series then collecting the similar terms, i.e., multiplying Eq. (3.46) with $\mathbf{H}_e$ in the left side and integrating it from 0 to θ_0 with respect to θ, we have

$$\overline{\mathbf{L}}_{sc} \begin{bmatrix} \mathbf{A} \\ \mathbf{B} \\ \mathbf{C} \end{bmatrix} + \overline{\mathbf{L}}_{af} \begin{bmatrix} \mathbf{a} \\ \mathbf{b} \\ \mathbf{c} \end{bmatrix} - \omega^2 \left(\overline{\mathbf{M}}_{sc} \begin{bmatrix} \mathbf{A} \\ \mathbf{B} \\ \mathbf{C} \end{bmatrix} + \overline{\mathbf{M}}_{af} \begin{bmatrix} \mathbf{a} \\ \mathbf{b} \\ \mathbf{c} \end{bmatrix} \right) = \mathbf{0} \tag{3.51}$$

where

$$\begin{aligned}
\overline{\mathbf{L}}_{sc} &= \int_0^{\theta 0} \mathbf{H}_e \mathbf{L}_{sc} d\theta \\
\overline{\mathbf{L}}_{af} &= \int_0^{\theta 0} \mathbf{H}_e \mathbf{L}_{af} d\theta \\
\overline{\mathbf{M}}_{sc} &= \int_0^{\theta 0} \mathbf{H}_e \mathbf{M}_{sc} d\theta \\
\overline{\mathbf{M}}_{af} &= \int_0^{\theta 0} \mathbf{H}_e \mathbf{M}_{af} d\theta \\
\mathbf{H}_e &= \mathbf{H}_{sc}^T = [\cos\lambda_0\theta, \ldots, \cos\lambda_m\theta, \ldots, \cos\lambda_M\theta]^T
\end{aligned} \tag{3.52}$$

Finally, combining Eqs. (3.50) and (3.51) results in

$$\left(\mathbf{K} - \omega^2 \mathbf{M}\right)[\mathbf{A} \quad \mathbf{B} \quad \mathbf{C}]^T = \mathbf{0} \tag{3.53}$$

where $\mathbf{K}$ is the stiffness matrix and $\mathbf{M}$ is the mass matrix. They are defined as

$$\begin{aligned}
\mathbf{K} &= \overline{\mathbf{L}}_{sc} - \overline{\mathbf{L}}_{af} \begin{bmatrix} \mathbf{L}_{af}^{\theta 0} \\ \mathbf{L}_{af}^{\theta 1} \end{bmatrix}^{-1} \begin{bmatrix} \mathbf{L}_{sc}^{\theta 0} \\ \mathbf{L}_{sc}^{\theta 1} \end{bmatrix} \\
\mathbf{M} &= \overline{\mathbf{M}}_{sc} - \overline{\mathbf{M}}_{af} \begin{bmatrix} \mathbf{L}_{af}^{\theta 0} \\ \mathbf{L}_{af}^{\theta 1} \end{bmatrix}^{-1} \begin{bmatrix} \mathbf{L}_{sc}^{\theta 0} \\ \mathbf{L}_{sc}^{\theta 1} \end{bmatrix}
\end{aligned} \tag{3.54}$$

Thus, the natural frequencies and modes of the beams under consideration can be determined easily by solving the standard characteristic equation.

3.3.2 *Weak Form Solution Procedure (Rayleigh-Ritz Procedure)*

Instead of seeking a solution in strong form as described in Sect. 3.3.1, all the expansion coefficients can be treated equally and independently as the generalized

coordinates and solved directly from the Rayleigh–Ritz technique, which is the focus of the current section.

For free vibration analysis, the Lagrangian energy functional (L) of beams can be defined in terms of the strain energy and kinetic energy functions as:

$$L = T - U_s - U_{sp} \tag{3.55}$$

Substituting Eqs. (3.31), (3.32) (3.35) and (3.39) into Eq. (3.55) and taking its derivatives with respect to each of the undetermined coefficients and making them equal to zero

$$\begin{aligned} &\frac{\partial L}{\partial \Xi} = 0 \quad \text{and} \quad \begin{cases} \Xi = A_m, B_m, C_m \\ m = 0, 1, 2, \ldots M \end{cases} \\ &\frac{\partial L}{\partial \Psi} = 0 \quad \text{and} \quad \Psi = a_1, a_2, b_1, b_2, c_1, c_2 \end{aligned} \tag{3.56}$$

a total of 3*(M + 3) equations can be obtained and they can be summed up in a matrix form as:

$$\left(\mathbf{K} - \omega^2 \mathbf{M}\right)\mathbf{G} = \mathbf{0} \tag{3.57}$$

where $\mathbf{K}$ is the stiffness matrix for the beam, and $\mathbf{M}$ is the mass matrix. They are defined as

$$\begin{aligned} \mathbf{K} &= \begin{bmatrix} \mathbf{K}_{uu} & \mathbf{K}_{uw} & \mathbf{K}_{u\theta} \\ \mathbf{K}_{uw}^T & \mathbf{K}_{ww} & \mathbf{K}_{w\theta} \\ \mathbf{K}_{u\theta}^T & \mathbf{K}_{w\theta}^T & \mathbf{K}_{\theta\theta} \end{bmatrix} \\ \mathbf{M} &= \begin{bmatrix} \mathbf{M}_{uu} & \mathbf{0} & \mathbf{M}_{u\theta} \\ \mathbf{0} & \mathbf{M}_{ww} & \mathbf{0} \\ \mathbf{M}_{u\theta}^T & \mathbf{0} & \mathbf{M}_{\theta\theta} \end{bmatrix} \end{aligned} \tag{3.58}$$

The explicit forms of submatrices $\mathbf{K}_{ij}$ and $\mathbf{M}_{ij}$ in the stiffness and mass matrices are listed in follow

$$\mathbf{K}_{uu} = \int_0^{\theta 0} \left\{ \frac{A_{11}}{R} \frac{\partial \mathbf{H}^T}{\partial \theta} \frac{\partial \mathbf{H}}{\partial \theta} + \frac{A_{55}}{R} \mathbf{H}^T \mathbf{H} \right\} d\theta + k^u_{\theta 0} \mathbf{H}^T \mathbf{H}|_{\theta=0} + k^u_{\theta 1} \mathbf{H}^T \mathbf{H}|_{\theta=\theta 0}$$

$$\mathbf{K}_{uw} = \int_0^{\theta 0} \left\{ \frac{A_{11}}{R} \frac{\partial \mathbf{H}^T}{\partial \theta} \mathbf{H} - \frac{A_{55}}{R} \mathbf{H}^T \frac{\partial \mathbf{H}}{\partial \theta} \right\} d\theta$$

$$\mathbf{K}_{u\theta} = \int_0^{\theta 0} \left\{ \frac{B_{11}}{R} \frac{\partial \mathbf{H}^T}{\partial \theta} \frac{\partial \mathbf{H}}{\partial \theta} - A_{55} \mathbf{H}^T \mathbf{H} \right\} d\theta$$

$$\mathbf{K}_{ww} = \int_0^{\theta 0} \left\{ \frac{A_{11}}{R} \mathbf{H}^T \mathbf{H} + \frac{A_{55}}{R} \frac{\partial \mathbf{H}^T}{\partial \theta} \frac{\partial \mathbf{H}}{\partial \theta} \right\} d\theta + k^w_{\theta 0} \mathbf{H}^T \mathbf{H}|_{\theta=0} + k^w_{\theta 1} \mathbf{H}^T \mathbf{H}|_{\theta=\theta 0}$$

$$\mathbf{K}_{w\theta} = \int_0^{\theta 0} \left\{ \frac{B_{11}}{R} \mathbf{H}^T \frac{\partial \mathbf{H}}{\partial \theta} + A_{55} \frac{\partial \mathbf{H}^T}{\partial \theta} \mathbf{H} \right\} d\theta$$

$$\mathbf{K}_{\theta\theta} = \int_0^{\theta 0} \left\{ \frac{D_{11}}{R} \frac{\partial \mathbf{H}^T}{\partial \theta} \frac{\partial \mathbf{H}}{\partial \theta} + A_{55} R \mathbf{H}^T \mathbf{H} \right\} d\theta + K^\theta_{\theta 0} \mathbf{H}^T \mathbf{H}|_{\theta=0} + K^u_{\theta 1} \mathbf{H}^T \mathbf{H}|_{\theta=\theta 0}$$

$$\mathbf{M}_{uu} = \mathbf{M}_{ww} = \int_0^{\theta 0} \overline{I_0} R \mathbf{H}^T \mathbf{H} d\theta$$

$$\mathbf{M}_{u\theta} = \int_0^{\theta 0} \overline{I_1} R \mathbf{H}^T \mathbf{H} d\theta$$

$$\mathbf{M}_{\theta\theta} = \int_0^{\theta 0} \overline{I_2} R \mathbf{H}^T \mathbf{H} d\theta \tag{3.59}$$

where

$$\mathbf{H} = [\, \mathbf{H}_{sc} \quad \mathbf{H}_{af} \,] = [\cos \lambda_0 \theta, \ldots, \cos \lambda_m \theta, \ldots, \cos \lambda_M \theta, P_1(\theta), P_2(\theta)] \tag{3.60}$$

G is a column vector which contains, in an appropriate order, the unknown expansion coefficients:

$$\mathbf{G} = [\, \mathbf{A} \quad \mathbf{a} \quad \mathbf{B} \quad \mathbf{b} \quad \mathbf{C} \quad \mathbf{c} \,]^T \tag{3.61}$$

Obviously, the vibration results can now be easily obtained by solving a standard matrix eigenproblem.

3.4 Laminated Beams with General Boundary Conditions

Vibration results of laminated straight and curved beams with general boundary conditions are given in this section. The isotropic beams are treated as special cases of laminated beams in the presentation. Natural frequencies and mode shapes for straight and curved beams with different boundary conditions, lamination schemes and geometry parameters are presented using both strong form and weak form solution procedures. The convergence of the solutions is studied and the effects of shear deformation and rotary inertia, deepness term $(1 + z/R)$ and beam parameters (boundary conditions, lamination schemes, geometry parameters and material properties) are investigated as well.

For the sake of simplicity, character strings CBT_w, CBT_s, $SDBT_w$ and $SDBT_s$ are introduced to represent the beam theories and methods used in the calculation (where subscripts w and s denote weak form and strong form solution procedures, respectively). In addition, a two-letter string is applied to indicate the end conditions of a beam, such as C-F denotes a beam with C and F boundary conditions at the boundaries $\theta = 0$ and $\theta = \theta_0$, respectively. Unless otherwise stated, the natural frequencies of the considered beams are expressed in the non-dimensional parameters as $\Omega = \omega L_\theta^2 \sqrt{12\rho/E_1 h^2}$ and the material properties of the beams are given as: $\mu_{12} = 0.25$, $G_{13} = 0.5E_2$ (where L_θ represents the span length of a curved beam, i.e., $L_\theta = R\theta_0$).

3.4.1 Convergence Studies and Result Verification

Table 3.3 shows the convergence studies made for the first six natural frequencies (Hz) of a moderately thick, two-layered laminated ([0°/90°]) curved beam with completely free (F-F) and clamped (C-C) boundary conditions. The geometry and material constants of the beam are given as: $R = 1$ m, $\theta_0 = 1$, $h/R = 0.1$, $E_2 = 10$ GPa, $E_1/E_2 = 10$, $\mu_{12} = 0.27$, $G_{13} = 5.5$ GPa, $\rho = 1{,}700$ kg/m^3. Both the $SDBT_w$ and $SDBT_s$ solutions for truncation schemes $M = 8, 9, 14, 15$ are included in studies. It is obvious that the modified Fourier series solution has an excellent convergence, and is sufficiently accurate even when only a small number of terms are included in the series expressions. In addition, from the table, we can see that the $SDBT_w$ solutions converge faster than the $SDBT_s$ ones. Unless otherwise stated, the truncation number (M) of the displacement expressions will be uniformly selected as $M = 15$ in the following calculation and the weak form solution procedure will be adopted in the calculation.

In Table 3.4, comparisons of the frequency parameters Ω for a two-layered, unsymmetrically laminated ([90°/0°]) curved beam with SD-SD boundary conditions are presented. The geometric properties of the layers of the beam are the same as those used in Table 3.3 except that the thickness-to-length ratio is given as

Table 3.3 Convergence of the first six natural frequencies (Hz) for a [0°/90°] laminated curved beam with F-F and C-C boundary conditions (R = 1 m, θ_0 = 1, h/R = 0.1)

Boundary conditions	M	Mode number					
		1	2	3	4	5	6
F-F	$SDBT_w$						
	8	123.88	314.88	549.83	813.20	895.85	1099.3
	9	123.88	314.84	549.78	812.30	895.63	1098.3
	14	123.88	314.81	549.63	811.86	895.58	1096.5
	15	123.88	314.81	549.63	811.84	895.57	1096.5
	$SDBT_s$						
	8	124.60	316.99	553.41	821.66	897.25	1109.4
	9	124.59	316.20	552.42	817.25	896.32	1106.3
	14	124.01	315.15	550.23	813.00	895.80	1098.0
	15	124.01	315.09	550.11	812.80	895.72	1097.7
C-C	$SDBT_w$						
	8	262.54	279.29	514.27	723.46	894.04	990.46
	9	262.53	279.27	514.07	723.31	893.95	987.46
	14	262.52	279.21	513.96	722.71	893.93	986.40
	15	262.52	279.21	513.95	722.71	893.93	986.34
	$SDBT_s$						
	8	262.84	280.27	517.05	729.92	895.50	1005.6
	9	262.74	279.86	516.23	727.91	894.55	996.79
	14	262.57	279.36	514.43	723.68	894.11	988.60
	15	262.56	279.33	514.34	723.58	894.04	987.94

Table 3.4 Comparison of the frequency parameters Ω for a [90°/0°] laminated curved beam with SD-SD boundary conditions (R = 1 m, θ_0 = 1)

h/L_θ	Qatu (1993)			$SDBT_w$		
	1	2	3	1	2	3
0.01	4.0094	18.000	41.286	4.0179	18.042	41.388
0.02	3.9885	17.839	40.681	3.9969	17.878	40.770
0.05	3.9109	17.089	37.667	3.9190	17.124	37.738
0.10	3.7419	15.329	31.300	3.7496	15.357	31.349
0.20	3.3312	11.808	21.481	3.3387	11.833	21.523

h/L_θ = 0.01, 0.02, 0.05, 0.1 and 0.2 and the elementally material parameters of the layers are: E_1/E_2 = 15. From the table, we can see that the present solutions agree very well with exact solutions published by Qatu (1993). The differences between the two results are very small, and do not exceed 0.27 % for the worst case. To further prove the validity of the present method, Table 3.5 lists comparisons of the frequency parameters Ω for a two-layered, unsymmetrically laminated ([90°/0°]) curved beam with various boundary conditions. The layers of the beam are thought

Table 3.5 Comparison of the frequency parameters Ω for a [90°/0°] laminated curved beam with different boundary conditions ($h/L_\theta = 0.01$, $R/L_\theta = 2$, $E_1/E_2 = 15$)

B.C.	Theory	Mode number				
		1	2	3	4	5
S-S	Qatu and Elsharkawy (1993)	18.434	37.935	74.549	99.888	143.10
	$SDBT_w$	18.448	37.910	74.303	99.435	142.01
	CBT_w	18.473	38.009	74.703	99.905	142.85
SD-SD	Qatu and Elsharkawy (1993)	4.5173	18.593	42.050	74.884	117.92
	$SDBT_w$	4.5249	18.606	42.009	74.632	116.37
	CBT_w	4.5268	18.631	42.137	75.037	117.32
C-C	Qatu and Elsharkawy (1993)	29.015	51.348	94.637	111.64	149.21
	$SDBT_w$	28.973	51.167	93.982	111.02	147.71
	CBT_w	29.076	51.436	94.833	111.35	149.17
C2-C2	Qatu and Elsharkawy (1993)	10.445	29.145	57.291	94.837	144.65
	$SDBT_w$	10.255	29.028	56.995	94.103	140.25
	CBT_w	10.467	29.205	57.406	95.008	141.98

to be of equal thickness and made from material with following properties: $h/L_\theta = 0.01$, $R/L_\theta = 2$, $E_1/E_2 = 15$. The Ritz solutions obtained by Qatu and Elsharkawy (1993) by using the classical beam theory are selected as the benchmark solutions. A consistent agreement between the present results and the referential data is seen from the table. Furthermore, comparing the sixth frequencies of the beam, we can see that the CBT solutions are less accurate in the higher modes. The maximum difference (in the sixth frequency parameters) between the $SDBT_w$ and CBT_w solutions can be 1.67 % for the worst case.

3.4.2 Effects of Shear Deformation and Rotary Inertia

In this section, effects of the shear deformation and rotary inertia which are neglected in the CBT will be investigated. Shear deformation was first applied in the analysis of beams by Timoshenko (1921). This effect is higher in composite materials since the longitudinal to shear modulus ratio is much higher in composites than metallic materials (Hajianmaleki and Qatu 2012b). Figures 3.5 and 3.6 show the differences between the lowest three frequency parameters Ω obtained by CBT_w and $SDBT_w$ for an isotropic curved beam and a two-layered, [0°/90°] laminated curved beam with different boundary conditions and thickness-to-span length ratios, respectively. Both F-F and C-C boundary conditions are shown in each figure. The geometric and material constants of the layers of the two beams are: $R/L_\theta = 1$, $E_1/E_2 = 1$(Fig. 3.5)

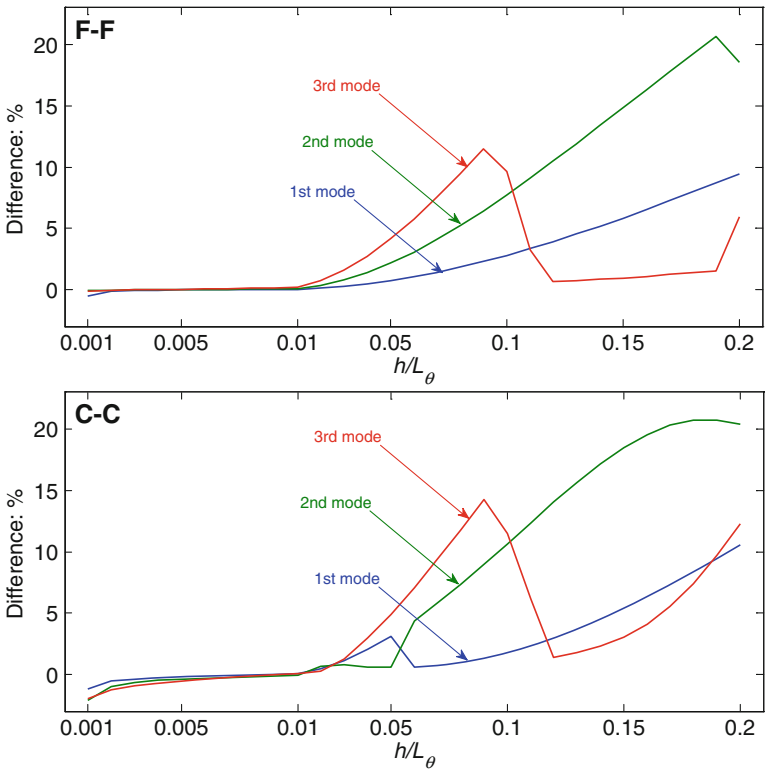

Fig. 3.5 Differences between the lowest three frequency parameters Ω obtained by CBT_w and $SDBT_w$ for an isotropic curved beam ($R/L_\theta = 1$, $E_1/E_2 = 1$)

and $E_1/E_2 = 15$ (Fig. 3.6). The thickness-to-span length ratio h/L_θ is varied from 0.001 to 0.2, corresponding to very thin to thick beams. From the figures, we can see that the effects of the shear deformation and rotary inertia increase as the orthotropy ratio (E_1/E_2) increases. Furthermore, when the thickness-to-span length ratio h/L_θ is less than 0.02, the maximum difference between the frequency parameters Ω obtained by CBT_w and $SDBT_w$ is less than 4 %. However, when the thickness-to-span length ratio h/L_θ is equal to 0.1, this difference can be as many as 11.5 % for the isotropic curved beam and 32.3 % for the [0°/90°] laminated one. As expected, it can be seen that the difference between the CBT_w and $SDBT_w$ solutions increases with thickness-to-span length ratio increases. Figure 3.6 also shows that the maximum difference between these two results can be as many as 50.4 % for a thickness-to-length ratio of 0.2. In such case, the CBT_w results are utterly inaccurate. This investigation shows that the CBT only applicable for thin beams. For beams with higher thickness ratios, both shear deformation and rotary inertia effects should be included in the calculation. These results can be used in establishing the limits of classical shell and plate theories as well.

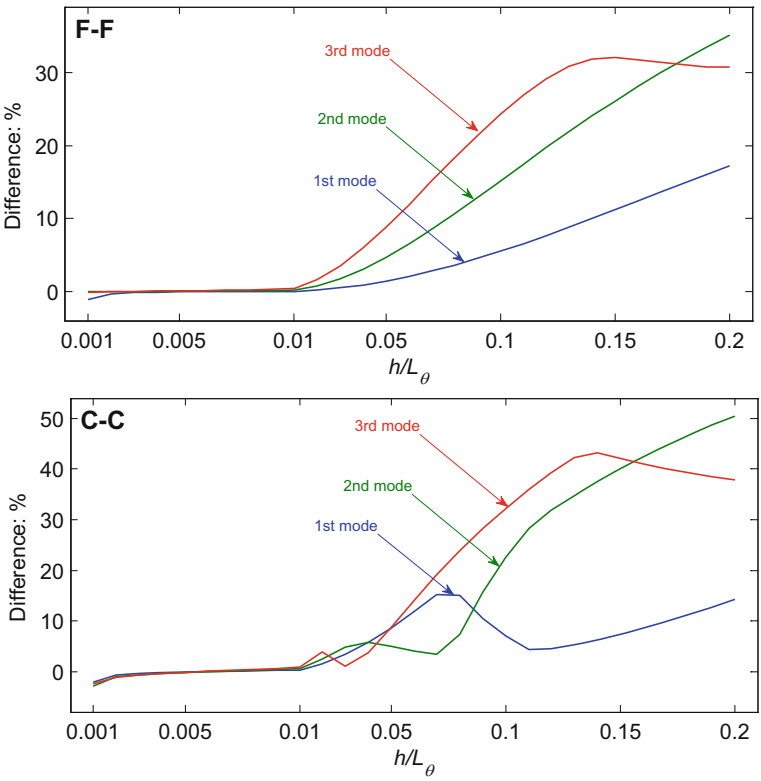

Fig. 3.6 Differences between the lowest three frequency parameters Ω obtained by CBT_w and $SDBT_w$ for a [0°/90°] laminated curved beam ($R/L_\theta = 1$, $E_1/E_2 = 15$)

3.4.3 Effects of the Deepness Term (1 + z/R)

Considering Eq. (3.23), the deepness term $(1 + z/R)$ introduces curvature complexity in the kinematic relations. When the thickness of the beam, h, is small compared to its radius of curvature R, i.e., $h/R << 1$ and $|z/R| << 1$, then deepness term $(1 + z/R)$ approximately equals to 1. In such case, the shear deformation shallow beam theories (SDSBT) can be obtained from the general SDBT (Khdeir and Reddy 1997; Qatu 1992). Qatu (2004) pointed out that this term should not be neglected in the analysis especially when the span length-to-radius ratio is more than 1/2. In this section, effects of the deepness term $(1 + z/R)$ will be investigated.

Neglecting the deepness term and including the effects of shear deformation and rotary inertia, the normal and shear strains at any point of a beam can be rewritten as:

$$\varepsilon_\theta = \varepsilon_\theta^0 + z\chi_\theta \quad \gamma_{\theta z} = \gamma_{\theta z}^0 \tag{3.62}$$

where the normal and shear strains in the reference surface (ε_θ^0 and $\gamma_{\theta z}^0$) and the curvature change (χ_θ) are given as in Eq. (3.24). Thus, the corresponding stress-strain relations in the kth layer of a laminated beam can be written as:

$$\left\{ \begin{array}{c} \sigma_\theta \\ \tau_{\theta z} \end{array} \right\}_k = \left[\begin{array}{cc} \overline{Q_{11}^k} & 0 \\ 0 & \overline{Q_{55}^k} \end{array} \right] \left\{ \begin{array}{c} \varepsilon_\theta \\ \gamma_{\theta z} \end{array} \right\}_k \tag{3.63}$$

By carrying the integration of the stresses over the cross-section, the force and moment resultants (N_θ, Q_θ and M_θ) become:

$$\left[\begin{array}{c} N_\theta \\ M_\theta \\ Q_\theta \end{array} \right] = \left[\begin{array}{ccc} A_{11} & B_{11} & 0 \\ B_{11} & D_{11} & 0 \\ 0 & 0 & A_{55} \end{array} \right] \left[\begin{array}{c} \varepsilon_\theta^0 \\ \chi_\theta \\ \gamma_{\theta z} \end{array} \right] \tag{3.64}$$

The stiffness coefficients A_{11}, B_{11} and D_{11} are given in Eq. (3.7) and A_{55} is defined as:

$$A_{55} = K_s b \sum_{k=1}^{N} \overline{Q_{11}^k}(z_{k+1} - z_k) \tag{3.65}$$

where K_s is the shear correction factor, typically taken at 5/6.

Substituting Eq. (3.64) into the energy functions of the beams (see, Sect. 3.2.3) and applying the Ritz solution procedure in the similar manner described before (see, Sect. 3.3.2), the vibration solutions of laminated beams in the framework of SDSBT can be obtained (represent by SDSBT_w). It should be stressed that the inertia terms of the beam in the SDSBT are defined as:

$$\begin{gathered} \overline{I_0} = I_0 \\ \overline{I_1} = I_1 \\ \overline{I_2} = I_2 \\ [I_0, I_1, I_2] = b \sum_{k=1}^{N} \int_{z_k}^{z_{k+1}} \rho^k [1, z, z^2] dz \end{gathered} \tag{3.66}$$

Figures 3.7and 3.8 show the differences between the lowest three non-dimensional frequency parameters Ω obtained by SDBT_w and SDSBT_w for a two layered, unsymmetrically laminated [0°/90°] curved beam and an isotropic curved beam with different span length-to-radius and thickness-to-radius ratios, respectively. The 'difference' is defined as: difference = (SDSBT_w − SDBT_w)/SDBT_w*100 %. The geometric and material constants of the layers of the beam are: R = 1, E_1/E_2 = 1 or

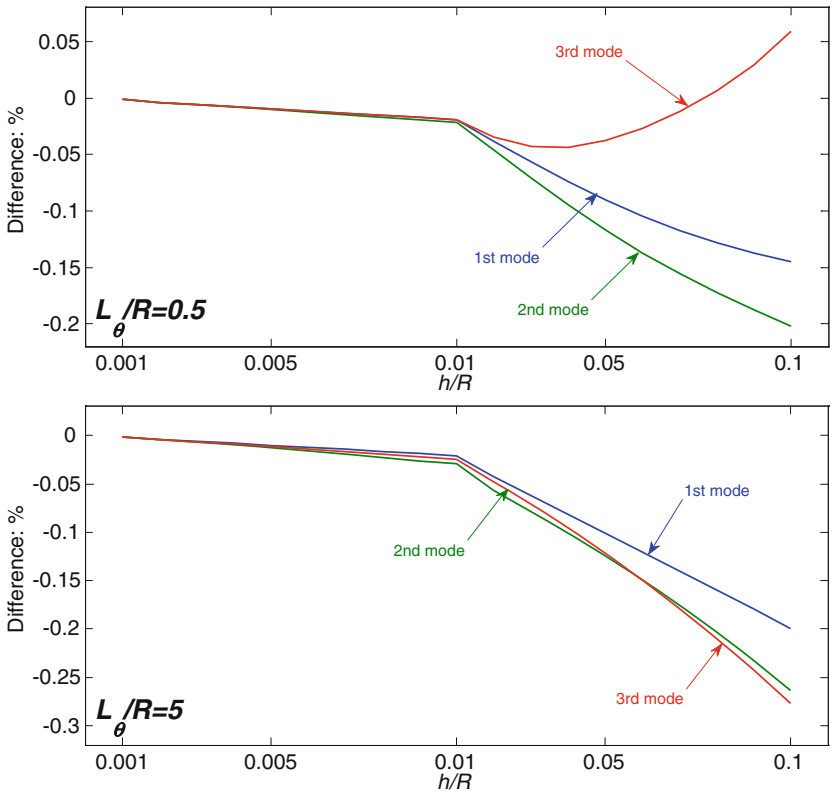

Fig. 3.7 Differences between the lowest three frequency parameters Ω obtained by $SDBT_w$ and $SDSBT_w$ for a [0°/90°] laminated curved beam (R = 1, E_1/E_2 = 15)

15 (laminated). The beams are assumed to be C-F supported. Two span length-to-radius ratios, i.e., L_θ/R = 0.5 and 5, corresponding to shallow and deep curved beams are shown in each figure. The thickness-to-radius ratio h/R is varied from 0.001 to 0.1. As expected, the effects of the deepness term increase as the thickness-to-radius ratio increases. The included angle θ_0 of the curved beam is the span length-to-radius ratio. This means that the span length-to-radius ratio of 5 indicates a very deep curved beam with an included angle of 286.48°, which are more than three quarters of the closed circle. In this case, the difference between the frequency parameters Ω obtained by $SDSBT_w$ and $SDBT_w$ is very small and the maximum difference is less than 0.41 % for the worst case. In addition, it is clear from the figures that the effects of the deepness term vary with mode number and span length-to-radius ratio and orthotropy ratio (E_1/E_2). In the case of span length-to-radius ratio L_θ/R = 5, the $SDBT_w$ results are generally higher than those of $SDSBT_w$. These results can be used in establishing the limits of shell theories and shell equations.

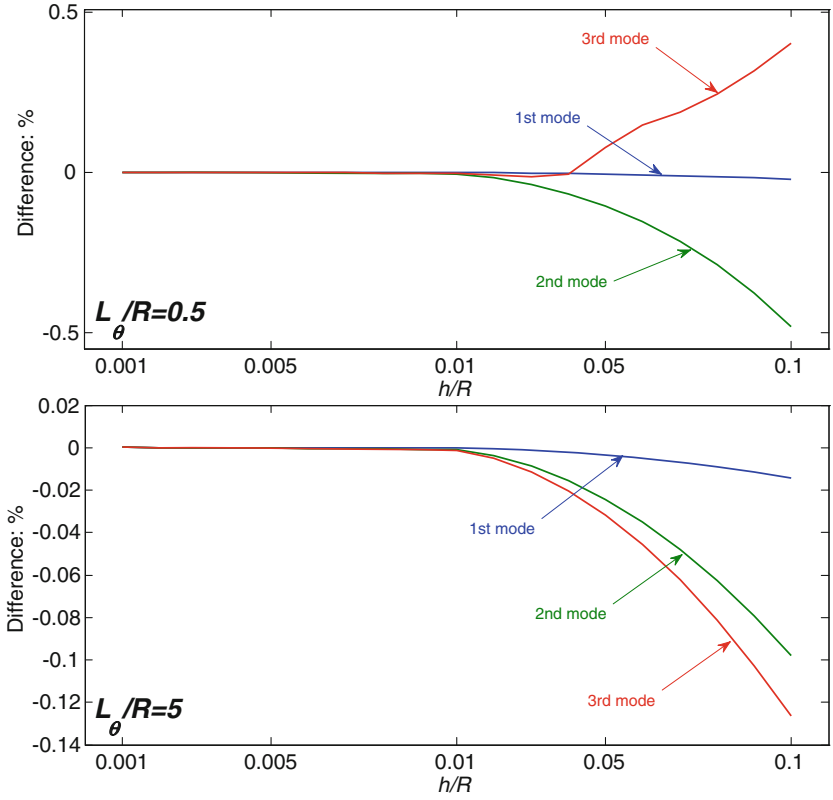

Fig. 3.8 Differences between the lowest three frequency parameters Ω obtained by $SDBT_w$ and $SDSBT_w$ for an isotropic curved beam ($R = 1$, $E_1/E_2 = 1$)

3.4.4 *Isotropic and Laminated Beams with General Boundary Conditions*

In this section, isotropic and laminated beams with various boundary conditions including the classical restraints and the elastic ones will be studied. Only the free vibration solutions (natural frequencies and mode shapes) based on SDBT and weak form solution procedure are considered in this section.

Table 3.6 shows the frequency parameters Ω obtained for a two-layered, [0°/90°] laminated curved beam with different thickness-to-radius ratios and various classical boundary conditions. The geometry and material parameters used in the study are: $R = 1$, $\theta_0 = 2\pi/3$, $E_1/E_2 = 15$. And the thickness-to-radius ratios performed in the study are $h/R = 0.01$, 0.05 and 0.1, corresponding to thin to moderately thick curved beams. The first observation is that the frequency parameters for curved beams with F-SD boundary conditions (no constraints on the in-plane displacement) are higher than those of curved beam with F-S boundary conditions.

Table 3.6 Frequency parameters Ω for a [0°/90°] laminated curved beam with different thickness-to-radius ratios and boundary conditions ($R = 1$, $\theta_0 = 2\pi/3$)

h/R	Mode	Boundary conditions							
		F-F	F-S	F-SD	F-C	S-S	SD-SD	S-C	C-C
0.01	1	9.5195	5.1928	5.6583	1.8539	14.614	2.1861	19.448	25.039
	2	27.392	20.523	21.455	7.7666	37.008	15.969	43.325	49.995
	3	55.452	46.358	47.226	25.569	71.295	39.538	80.689	90.812
	4	93.083	81.757	82.608	53.771	113.13	72.651	124.27	135.87
	5	140.16	126.70	127.44	91.461	166.27	115.27	180.51	195.52
0.05	1	9.5681	5.2531	5.6975	1.8445	14.878	2.2102	19.435	24.690
	2	27.523	20.756	21.581	7.7620	37.546	16.093	42.965	48.220
	3	55.053	46.447	47.003	25.389	70.686	39.438	78.179	86.441
	4	90.949	80.485	80.920	52.785	110.31	71.371	117.75	124.06
	5	134.28	122.32	122.47	87.966	157.68	111.09	165.51	176.82
0.1	1	9.6198	5.3307	5.7443	1.8487	14.964	2.2341	18.948	23.492
	2	27.102	20.648	21.357	7.7249	36.701	16.008	40.390	43.401
	3	52.379	44.743	45.037	24.451	65.996	38.040	70.061	75.703
	4	83.207	74.347	74.565	49.195	92.469	66.257	94.377	94.698
	5	117.69	108.20	108.23	78.109	99.117	98.930	108.30	121.93

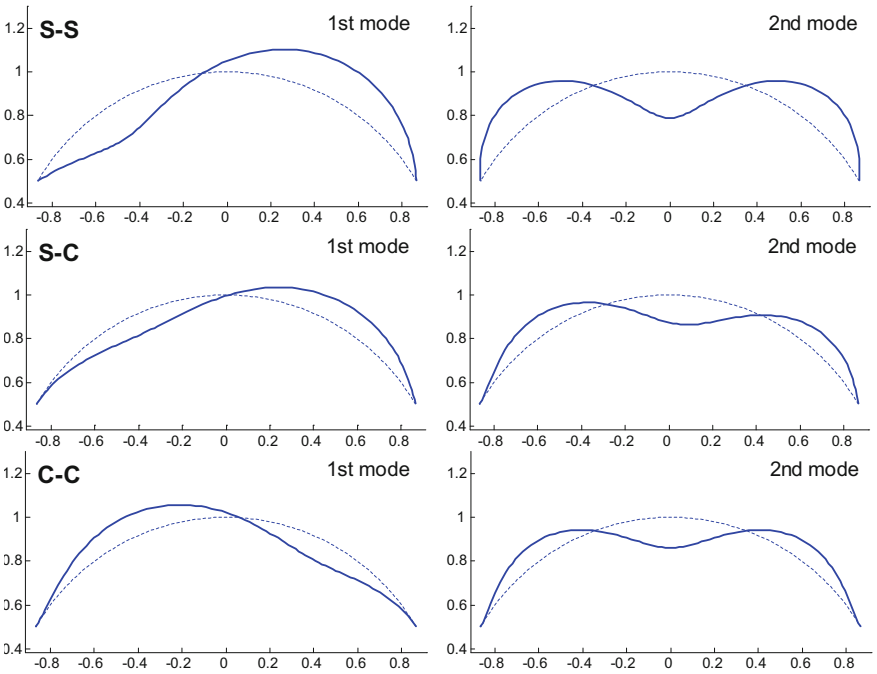

Fig. 3.9 The lowest three mode shapes for a moderately *thick* (h/R = 0.05), [0°/90°] laminated curved beam with different boundary conditions (R = 1, $\theta_0 = 2\pi/3$)

The second observation is that the fundamental frequency parameter of the beam increases with thickness-to-radius ratio increases when subjected to F-F, F-S, F-SD, S-S and SD-SD boundary conditions. In other cases, the beam frequency parameters decrease with thickness-to-radius ratio increases. In Fig. 3.9, the lowest two mode shapes for the beam with thickness-to-radius ratio h/R = 0.05 are presented for S-S, S-C and C-C boundary conditions, respectively. These mode shapes are determined by substituting the related eigenvectors into the assumed displacement expansions.

Table 3.7 studies the effects of the orthotropy ratio (E_1/E_2) on the frequency parameters Ω for a two-layered, [0°/90°] laminated curved beam with different boundary conditions. The geometry parameters used in the investigation are: R = 1, $\theta_0 = 2\pi/3$, h/R = 0.05. Four different orthotropy ratios considered in the investigation are: E_1/E_2 = 1, 10, 20 and 40. From the table, we can see that the increment in the orthotropy ratio results in decreases of the frequency parameters.

Since the effects of both shear deformation and rotary inertia and the deepness term are included in the SDBT, therefore, it can be applied to predict vibration characteristics of moderately thick curved beams with arbitrary included angles. Table 3.8 shows the frequency parameters Ω obtained for a two-layered, [0°/90°]

Table 3.7 Frequency parameters Ω for a [0°/90°] laminated curved beam with different orthotropy ratios and boundary conditions (R = 1, $\theta_0 = 2\pi/3$, h/R = 0.05)

E_1/E_2	Mode	Boundary conditions							
		F-F	F-S	F-SD	F-C	S-S	SD-SD	S-C	C-C
1	1	20.400	11.119	12.142	3.969	31.287	4.7104	41.488	53.239
	2	58.737	43.932	46.030	16.555	78.374	34.295	91.007	103.85
	3	118.35	98.751	100.92	54.567	150.95	84.576	169.72	189.98
	4	197.48	172.94	175.47	113.83	231.46	154.54	245.55	254.89
	5	295.26	265.45	268.86	191.89	310.10	243.48	315.43	328.61
10	1	10.504	5.7639	6.2542	2.0255	16.332	2.4261	21.377	27.203
	2	30.248	22.797	23.714	8.527	41.263	17.681	47.317	53.219
	3	60.628	51.111	51.750	27.941	77.959	43.411	86.432	95.797
	4	100.42	88.810	89.326	58.211	121.95	78.764	130.29	137.23
	5	148.74	135.41	135.62	97.288	175.12	122.98	183.35	197.31
20	1	9.0415	4.9652	5.3841	1.7430	14.052	2.0888	18.327	23.246
	2	25.977	19.597	20.372	7.329	35.409	15.194	40.445	45.305
	3	51.862	43.773	44.287	23.931	66.471	37.166	73.360	80.937
	4	85.465	75.661	76.056	49.652	103.46	67.098	110.27	116.08
	5	125.82	114.65	114.78	82.521	147.35	104.14	154.61	164.50
40	1	8.1490	4.4770	4.8532	1.5721	12.623	1.8833	16.375	20.657
	2	23.301	17.591	18.282	6.584	31.598	13.642	35.852	39.892
	3	46.183	39.014	39.462	21.360	58.749	33.140	64.359	70.464
	4	75.416	66.816	67.161	43.956	90.500	59.296	95.798	100.33
	5	109.88	100.19	100.31	72.335	127.43	91.082	133.01	140.01

Table 3.8 Frequency parameters Ω for a [0°/90°] laminated curved beam with different included angles and boundary conditions (R = 1, h/R = 0.05)

θ_0	Mode	Boundary conditions							
		F-F	F-S	F-SD	F-C	S-S	SD-SD	S-C	C-C
π/2	1	10.005	5.9054	6.3409	1.7722	16.561	3.2096	20.938	26.105
	2	28.178	21.953	22.468	8.586	38.863	17.248	43.534	47.549
	3	55.053	47.152	47.364	26.473	70.658	40.139	76.711	84.959
	4	89.297	79.705	79.831	53.088	106.03	70.809	106.34	106.36
	5	129.63	118.68	118.70	86.151	108.37	108.12	121.43	136.93
π	1	8.7706	4.3969	4.5494	2.0633	10.931	12.841	15.543	20.777
	2	25.365	17.744	18.975	6.569	33.468	36.216	39.449	45.584
	3	52.896	43.201	44.337	22.381	67.002	69.019	75.214	83.912
	4	89.877	78.130	79.207	49.875	108.64	110.69	118.03	127.44
	5	135.61	122.09	122.91	86.475	159.48	160.71	170.57	182.12
3π/2	1	8.2428	3.9844	4.1003	2.6458	5.1157	3.2921	9.8808	14.992
	2	21.531	13.115	14.420	5.8982	25.651	6.6963	32.026	38.680
	3	47.428	36.490	38.078	17.548	57.966	28.905	66.578	75.602
	4	84.055	70.815	72.626	43.413	100.26	61.559	110.72	121.60
	5	130.50	115.27	116.99	79.703	152.25	103.92	164.70	177.47

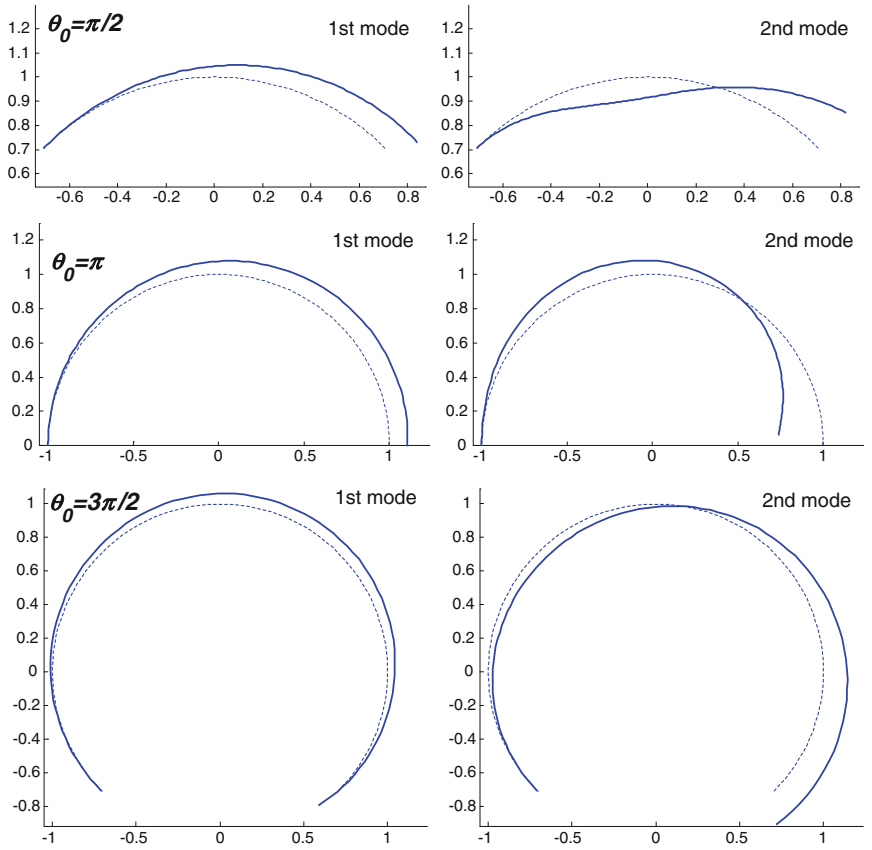

Fig. 3.10 The lowest two mode shapes for a [0°/90°] laminated curved beam with F-C boundary conditions and different included angles (R = 1, h/R = 0.05)

laminated curved beam with different included angles and various combinations of classical boundary conditions. The geometry and material parameters of the beam are assumed to be: R = 1, h/R = 0.05, E_1/E_2 = 15. It can be seen from the table that in all the boundary condition cases, all the frequency parameters of the beam decrease with included angle increases. It may be attributed to the stiffness of the curved beam reduces when the included angle increases. In order to enhance our understanding of the effects of the included angle, Fig. 3.10 presents the lowest two mode shapes of the beam with F-C boundary conditions. From the figure, we can see that the influence of the included angle on the mode shapes of the beam varies with mode sequence.

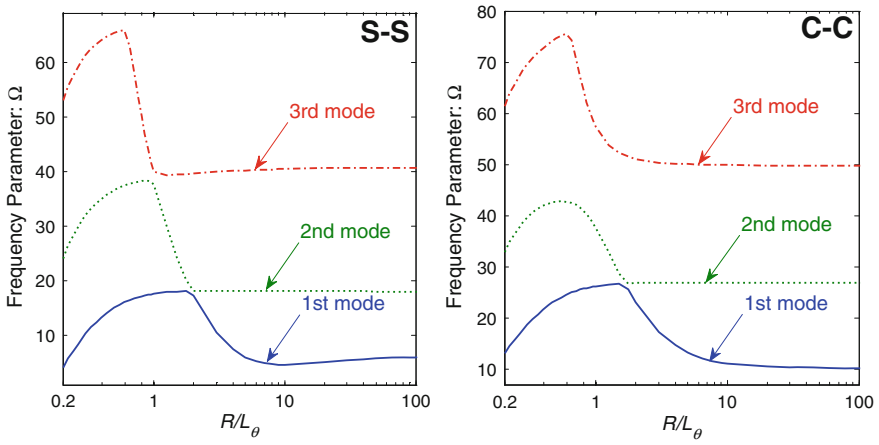

Fig. 3.11 Variation of frequency parameters Ω versus radius-to-span length ratio (R/L_θ) for a [0°/90] laminated curved beam with S-S and C-C boundary conditions ($h/L_\theta = 0.05$)

Then, influence of the radius-to-span length ratio (R/L_θ) on the frequencies of a [0°/90°] laminated curved beam ($E_1/E_2 = 15$) is investigated. The beam is made from composite layers with following geometry constants: $L_\theta = 1$, $h/L_\theta = 0.05$. Figure 3.11 shows variations of the lowest three frequency parameters Ω versus the radius-to-span length ratio for the beam with S-S and C-C boundary conditions. Increasing the radius-to-span length ratio from 0.2 (very deep curved beam) to 10 (shallow curved beam), the effects of the radius-to-span length ratio are very large for the frequency parameters. We can see clearly that the frequency parameter trace of the fundamental modes climb up and then decline, and reach its crest around $R/L_\theta = 2$. The same tendency can be seen in the second and third modes as well while the second and third ones reach their crests around $R/L_\theta = 1$ and $R/L_\theta = 0.8$. The similar characteristics can be found in the right subfigure. When the radius-to-span length ratio is increased from 10 to 100, increasing the radius-to-span length ratio has very limited influence on the frequency parameters due to the curved beam is very shallow and its vibration behaviors approximate to a straight beam.

Finally, Table 3.9 shows the first three frequency parameters Ω for a [−45°/45°] laminated curved beam ($L_\theta = 1$, $h/L_\theta = 0.05$, $E_1/E_2 = 15$) with different radius-to-span length ratios and elastic boundary conditions. The radius-to-span length ratios included in the calculation are $1/\pi$, $4/\pi$ and ∞. The radius-to-span length ratio of $1/\pi$ and $4/\pi$ correspond to curved beam with an included angle of π and π/4, respectively. The last radius-to-span length ratio of ∞ corresponds to a straight

Table 3.9 The first three frequency parameters Ω for a [−45°/45°] laminated curved beam with different radius-to-span length ratios and S-Elastic boundary conditions (L_θ = 1, h/L_θ = 0.05)

R/L_θ	Γ	$k_{\theta 1}^u=\Gamma, k_{\theta 1}^w=10^7D, K_{\theta 1}^\theta=0$			$k_{\theta 1}^u=0, k_{\theta 1}^w=10^7D, K_{\theta 1}^\theta=\Gamma$		
		1	2	3	1	2	3
1/π	$10^{-1}D$	0.4465	12.851	36.277	0.6846	12.974	36.380
	$10^{0}D$	1.4104	12.863	36.280	1.8096	13.816	37.125
	$10^{1}D$	4.4087	12.992	36.314	2.8424	15.779	39.292
	$10^{2}D$	10.805	16.473	36.709	3.0734	16.507	40.291
	$10^{3}D$	11.828	32.677	49.626	3.0996	16.600	40.426
	$10^{4}D$	11.887	34.153	64.561	3.1022	16.610	40.440
4/π	$10^{-1}D$	4.6699	20.169	43.834	4.7857	20.328	43.957
	$10^{0}D$	4.7105	20.169	43.835	5.4645	21.404	44.860
	$10^{1}D$	5.0975	20.169	43.844	6.5092	23.900	47.523
	$10^{2}D$	7.8777	20.170	43.932	6.7873	24.804	48.738
	$10^{3}D$	17.166	20.189	44.503	6.8198	24.918	48.902
	$10^{4}D$	20.147	25.119	45.374	6.8231	24.929	48.918
∞ (straight)	$10^{-1}D$	5.4235	20.949	44.711	5.5870	21.101	44.843
	$10^{0}D$	5.4235	20.949	44.711	6.5033	22.146	45.818
	$10^{1}D$	5.4235	20.949	44.711	7.8962	24.625	48.748
	$10^{2}D$	5.4234	20.949	44.711	8.2619	25.535	50.111
	$10^{3}D$	5.4236	20.949	44.711	8.3044	25.649	50.295
	$10^{4}D$	5.4234	20.949	44.711	8.3087	25.661	50.314

beam. The beam is simply-supported at the edge of $\theta = 0$ and elastically restrained at the other edge (S-Elastic). Table 3.10 shows similar studies for the C-Elastic boundary conditions. The tables show that increasing the axial restrained rigidity has very limited effects on the straight beam. It is attributed to the lower frequency parameters of a straight beam are dominated by its transverse vibration.

In conclusion, vibration of isotropic and laminated straight and curved beams is studied in this chapter. The effects of shear deformation and rotary inertia, deepness term $(1 + z/R)$ and other beam parameters are clearly outlined. It is shown that the difference (for the lowest three frequency parameters) between the CBT and SDBT solutions increases with thickness-to-length ratio increases. For a laminated curved beam (R/L_θ = 1, E_1/E_2 = 15, [0°/90°] lamination scheme) with thickness-to-length ratios of 0.05, 0.1, 0.15 and 0.2, the maximum differences can be as many as 8.8, 32.3, 42 and 50.4 % for the worst case, respectively. The effects of the deepness term $(1 + z/R)$ on the frequency parameters is very small, the maximum difference between the frequency parameters Ω obtained by SDSBT (neglect the deepness term) and SDBT is less than 0.41 % for the worse case of a curved beam of span length-to-radius ratio L_θ/R = 5 and thickness-to-radius ratio h/R = 0.1. A variety of

Table 3.10 The first three frequency parameters Ω for a [−45°/45°] laminated curved beam with different radius-to-span length ratios and C-Elastic boundary conditions (L_θ = 1, h/L_θ = 0.05)

R/L_θ	Spring rigidity	$k_{\theta 1}^{u}=\Gamma, k_{\theta 1}^{w}=10^7 D, K_{\theta 1}^{\theta}=0$			$k_{\theta 1}^{u}=0, k_{\theta 1}^{w}=10^7 D, K_{\theta 1}^{\theta}=\Gamma$		
		1	2	3	1	2	3
1/π	$10^{-1}D$	3.0784	17.040	40.988	3.0752	17.181	41.080
	$10^{0}D$	3.3805	17.045	40.991	3.2670	18.139	41.756
	$10^{1}D$	5.5452	17.094	41.022	3.5970	20.410	43.784
	$10^{2}D$	13.775	18.337	41.374	3.6929	21.272	44.749
	$10^{3}D$	16.321	35.923	51.778	3.7044	21.382	44.882
	$10^{4}D$	16.397	38.427	69.273	3.7055	21.394	44.895
4/π	$10^{-1}D$	7.5129	24.694	48.910	7.6416	24.848	49.019
	$10^{0}D$	7.5373	24.694	48.912	8.4238	25.915	49.821
	$10^{1}D$	7.7754	24.695	48.929	9.7649	28.553	52.224
	$10^{2}D$	9.7491	24.703	49.084	10.149	29.564	53.331
	$10^{3}D$	17.734	24.797	49.989	10.195	29.693	53.480
	$10^{4}D$	23.782	26.081	51.044	10.200	29.706	53.495
∞ (straight)	$10^{-1}D$	8.3092	25.662	50.316	8.4796	25.807	50.442
	$10^{0}D$	8.3092	25.662	50.316	9.4924	26.822	51.368
	$10^{1}D$	8.3092	25.662	50.316	11.219	29.395	54.250
	$10^{2}D$	8.3092	25.662	50.316	11.710	30.398	55.641
	$10^{3}D$	8.3092	25.662	50.316	11.768	30.526	55.832
	$10^{4}D$	8.3092	25.662	50.316	11.774	30.539	55.851

new vibration results including frequencies and mode shapes for straight and curved laminated beams with classical and elastic restraints as well as different geometric and material parameters are given, which may serve as benchmark solutions for the future researches.